HHS Public Access

Author manuscript

Acta Neuropathol. Author manuscript; available in PMC 2018 July 01.

Published in final edited form as:

Acta Neuropathol. 2017 July ; 134(1): 65–78. doi:10.1007/s00401-017-1679-9.

Expansion of the classification of FTLD-TDP: distinct pathology associated with rapidly progressive frontotemporal degeneration

Edward B. Lee[1,2,3], **Sílvia Porta**[2,3], **G. Michael Baer**[4], **Yan Xu**[2,3], **EunRan Suh**[2,3], **Linda K. Kwong**[2,3], **Lauren Elman**[4], **Murray Grossman**[4], **Virginia M.-Y. Lee**[2,3], **David J. Irwin**[4], **Vivianna M. Van Deerlin**[2,3], and **John Q. Trojanowski**[2,3]

[1]Translational Neuropathology Research Laboratory, Department of Pathology and Laboratory Medicine, Perelman School of Medicine, University of Pennsylvania, 613A Stellar Chance Laboratories, 422 Curie Blvd, Philadelphia, PA 19104, USA

[2]Center for Neurodegenerative Disease Research, University of Pennsylvania, Philadelphia, PA, USA

[3]Department of Pathology and Laboratory Medicine, University of Pennsylvania, Philadelphia, PA, USA

[4]Department of Neurology, University of Pennsylvania, Philadelphia, PA, USA

Abstract

Frontotemporal lobar degeneration with TDP-43 inclusions (FTLD-TDP) can typically be categorized into one of four distinct histopathologic patterns of TDP-43 pathology, types A to D. The strength of this histopathologic classification lies in the association between FTLD-TDP subtypes and various clinical and genetic features of disease. Seven cases of FTLD-TDP were identified here which were difficult to classify based on existing pathologic criteria. Distinct features common to these cases included TDP-43 aggregates over a wide neuroanatomic distribution comprised of granulofilamentous neuronal inclusions, abundant grains, and oligodendroglial inclusions. TDP-43 aggregates were phosphorylated and associated with loss of normal nuclear TDP-43 protein (nuclear clearance) but were negative for ubiquitin. Biochemical analysis confirmed the presence of insoluble and phosphorylated TDP-43 and also revealed a distinct pattern of TDP-43 C-terminal fragments relative to other FTLD-TDP subtypes. Finally, these cases were uniformly associated with a very rapid clinical course culminating in death within ~3 years of disease onset. We suggest that these cases may represent a unique clinicopathologic subtype of FTLD-TDP which we provisionally call “type E.” The immature appearance of TDP-43 aggregates, widespread distribution, uniform biochemical profile and rapid clinical course highlights the clinical and pathologic variability within FTLD-TDP, and raises the possibility that type E neuropathology is the sequelae of a particularly virulent strain of TDP-43 proteinopathy.

Electronic supplementary material The online version of this article (doi:10.1007/s00401-017-1679-9) contains supplementary material, which is available to authorized users.

Introduction

Frontotemporal lobar degeneration (FTLD) with TDP-43 inclusions (FTLD-TDP) exhibits considerable pathologic, clinical and genetic heterogeneity [16]. Patients may manifest the disease with a broad spectrum of clinical signs and symptoms ranging from behavioral/executive dysfunction with or without motor neuron disease (MND) to language dysfunction including semantic and nonfluent/agrammatic variants of primary progressive aphasia (PPA) [16]. Moreover, 20–40% of FTLD-TDP cases are associated with a family history of neurodegenerative disease, in part due to a high proportion of cases associated with disease-causing mutations [13, 24, 30, 37].

Pathologically, brain and spinal cord regions that degenerate in FTLD-TDP exhibit predominantly cytoplasmic or neuritic, insoluble, and phosphorylated TDP-43 aggregates in neurons and glia [2, 29]. These neuronal cytoplasmic TDP-43 aggregates are associated with loss of normal nuclear TDP-43 [29]. TDP-43 pathology is also seen in upper and lower motor neurons in nearly all cases of amyotrophic lateral sclerosis (ALS) [1, 4, 29]. Despite these unifying features, there is considerable pathologic heterogeneity in the distribution and morphology of TDP-43 aggregates in TDP-43 proteinopathies. Two independent studies identified distinct histopathologic patterns of TDP-43 pathology in FTLD-TDP [21, 31]. These studies predated the identification of TDP-43 protein as the main constituent of inclusions in FTLD and ALS, and thus relied on typing cases via immunohistochemistry using ubiquitin or type-specific antibodies. However, subsequent studies found a high concordance between ubiquitin and TDP-43 immunohistochemistry profiles for these pathological subtypes, thereby validating the presence of four distinct histopathologic subtypes of FTLD-TDP [7].

Important clinical and pathologic associations were made regarding the four subtypes [6, 9, 10, 17, 21, 22, 28, 31], prompting harmonization of the FTLD-TDP classification into types A to D [22]. Type A cases are associated with behavioral variant frontotemporal degeneration (bvFTD) or nonfluent/agrammatic PPA (naPPA), together with disease-causing mutations in *GRN*. Type B cases are associated with bvFTD including cases with MND, together with disease-causing mutations in *C9orf72*. Type C cases are associated with bvFTD or semantic variant PPA (svPPA). Type C cases are typically sporadic FTD having no association with any known disease-causing genetic mutations. Finally, type D histopathology is associated with mutation in valosin-containing protein (*VCP*) that cause familial inclusion body myositis, Paget's disease of bone, FTD, and/or ALS—variably called either IBMPFD-ALS or multisystem proteinopathy [9, 28].

We identified here seven cases of FTLD-TDP which could not be subtyped based on the harmonized pathologic criteria for FTLD-TDP types [22]. Examination of these cases revealed a distinct pattern of TDP-43 pathology with a surprisingly wide neuroanatomic distribution. Moreover, these cases were associated with a very rapid clinical course from onset to death. We propose that these cases may represent a unique, particularly virulent subtype of FTLD-TDP which we provisionally have designated "type E."

Materials and methods

Neuropathologic and clinical analyses

Neuropathologic analysis for cases #1–6 (Table 1) was performed according to the standardized procedures of the Center for Neurodegenerative Disease Research (CNDR) Brain Bank at the University of Pennsylvania as previously described [33]. Case #7 was obtained from the archives of the Hospital of the University of Pennsylvania and was largely processed in the same fashion except for a longer fixation period (~2 weeks). Briefly, brain and spinal cord regions were fixed in neutral buffered formalin, and 6 μm thick sections were cut from paraffin-embedded tissue. CNS tissue samples were obtained from the following regions for study here: mid-frontal cortex, primary motor cortex, superior and middle temporal cortex, parietal cortex (angular gyrus), occipital (primary visual) cortex, anterior cingulate gyrus, amygdala with parahippocampal gyrus, striatum and globus pallidus, mid-thalamus, hippocampus with parahippocampal gyrus, cerebellum including dentate nucleus, midbrain including substantia nigra, pons including locus ceruleus, medulla including inferior olive, and cervical spinal cord.

Closely adjacent series of sections from each CNS region were stained with hematoxylin and eosin or by immunohistochemistry using standard avidin–biotin complex methods with microwave antigen retrieval in citrate buffer. Antibodies included anti-TDP-43 antibodies (rat monoclonal TAR5P-1D3 (pS409/410 TDP-43) Ascenion, Munich, Germany [26]; 6H6E12, ProteinTech, Chicago, IL; 5104, 5095 and C1039, CNDR [18]), anti-ubiquitin (MAB1510, Chemicon, Temecula, CA, USA), anti-Aβ (NAB228, CNDR [19, 20]), anti-phosphorylated tau (PHF1, gift of Professor Peter Davies, Albert Einstein College of Medicine, New York, NY, USA), and anti-α-synuclein (SYN303, CNDR [11]). Antibody concentration optimization was sometimes required to enhance visualization of TDP-43 pathology.

Additional FTLD-TDP cases with documentation of age of onset, age of death, and FTLD-TDP subtype were identified in the CNDR Integrated Neurodegenerative Disease Database (INDD) as described [33]. 102 cases were identified corresponding to 38 type A, 34 type B, and 30 type C cases.

Immunofluorescence analysis

Double immunofluorescence was performed on formalin-fixed, paraffin-embedded tissue sections. Primary antibodies were incubated overnight at 4 °C in a humidified chamber (anti-ubiquitin, MAB1510; anti-TDP-43, rabbit polyclonal C1039, CNDR; anti-SQSTM1/p62, mouse monoclonal 2C11, Abnova, Walnut, CA; rabbit polyclonal, TIP-PTD-P01, Cosmo Bio Co., Carlsbad, CA, USA). Sections were washed in 0.1 M Tris buffer and then incubated with species-specific secondary antibodies for 2 h at room temperature (Alexa Fluor 594-conjugated goat anti-rabbit IgG; Alexa Fluor 488-conjugated goat anti-mouse IgG; Molecular Probes, Eugene, OR, USA). Sections were mounted in Vectashield-hard set medium containing DAPI (Vector Laboratories, Burlingame, CA, USA). Z-stack confocal images were obtained using a Lecia TCS SPE laser scanning confocal microscope and are presented as maximum intensity projections.

Genetic analysis

Genomic DNA was extracted from frozen brain tissue using commercial reagents (Qiagen, Germantown, MD, USA). All cases were screened for mutations associated with FTD and related neurodegenerative diseases using a custom targeted multi neurodegenerative disease sequencing panel (MiND-Seq), which covered the coding regions of 45 genes including but not limited to *MAPT*, *GRN*, *VCP*, *TARDBP*, *CHMP2B*, *SQSTM1*, *UBQLN2*, *CSF1R*, *PSEN1*, *SOD1*, *ATXN2*, *COQ2*, *NEFH*, *SETX, SPG11, ATP13A2, DNAJC13, DAO, EWSR1, LRRK2, PARK7, TMEM106B*, and *OPTN* [33]. Briefly, the panel uses next-generation sequencing technology with capture using Haloplex enrichment custom kit (Agilent, Wilmington, DE, USA) according to the manufacturer's protocol and sequencing on a Mi-Seq or Hi-Seq instrument (Illumina, San Diego, CA, USA). Alignment of sequence reads and variant calling were assessed by SureCall software (Agilent). In addition, cases were tested for the *C9orf72* hexanucleotide repeat expansion as previously described [32].

Biochemical analysis

Grey matter from frozen human post-mortem frontal cortex was sequentially extracted in a series of buffers of increasing strength, modified from a previously described procedure [29]. Tissue was sequentially extracted at 5 mL/g tissue with high-salt buffer containing 1% Triton X-100 (HS-TX; 10 mM Tris–HCl, pH 7.4, 0.5 M NaCl, 2 mM EDTA, 10% sucrose (w:v), 1% Triton X-100 (v:v), and 1 mM DTT) and a cocktail of protease/phosphatase inhibitors. Homogenates were centrifuged at 180,000*g* for 30 min at 4 °C and the pellet was resuspended in HS-TX buffer with additional 20% sucrose to remove myelin post-centrifugation. The remaining pellet was gently homogenized in nuclease buffer (50 mM Tris–HCl, pH 8.0, 20 mM NaCl, 5 mM MgCl2; 1 mL/g tissue) and treated with Bit-Nuclease (500 U/g tissue, Biotool Co, Houston, TX) on ice for 30 min before extraction with HS buffer containing 2% sarkosyl. The resulting pellet was washed in PBS (3.0 mL/g tissue) and then resuspended in PBS (0.1 mL/g tissue) by sonication (20–60 pulses at ~0.5 s/pulse, 2.5 intensity) using a hand-held probe (QSonica, Newtown, CT, USA). Proteins from this final fraction were separated on 12% Bis–Tris gels (NuPAGE Novex, Thermo Scientific, Rockford, IL, USA) in MOPS-SDS running buffer (Thermo Scientific). Proteins were transferred to 0.45 μM nitrocellulose membranes and blocked with Odyssey blocking buffer (LI-COR Biotechnology, Lincoln, NE, USA). Membranes were immunoblotted overnight at 4 °C with two pairs of primary antibodies diluted in Odyssey blocking buffer: anti-TDP-43 (mouse monoclonal, 5104, CNDR) and anti-p409/410-TDP-43 (rabbit polyclonal, TIP-PTD-P01, Cosmo Bio Co.); or anti-TDP-43 (rabbit polyclonal, 10782-2-AP, Proteintech, Chicago, IL, USA) and anti-p409/410-TDP-43 (rat monoclonal, TAR5P-1D3). After three washes in tris buffered saline with 0.1% Tween, membranes were further incubated with the corresponding pair of secondary antibodies: IRDye 680RD goat anti-mouse IgG (926-32210, LI-COR) and IRDye 800CW goat anti-rabbit IgG (926-32211, LI-COR); or IRDye 680RD goat anti-rabbit (926-68071, LI-COR) and IRDye 800RD affinity purified goat anti-rat IgG (612-132-003, LI-COR). Membranes were scanned using an ODY-2816 Imager and analyzed using Image Studio Software.

Statistical analysis

Basic summary statistics are reported including mean and standard deviation. Univariate linear regressions were performed using the R statistical package to determine the relationship between clinical measures (disease duration, age of death, age of onset) with histologic subtype and reported with β coefficient, standard error and *p* value. Type C cases which represent typical sporadic FTLD-TDP cases were chosen as the reference group for regressions.

Results

Six of the seven cases were characterized by a prominent social disorder and a clinical diagnosis of bvFTD, including one case with coexisting MND (Table 1). Two patients (cases #1 and 6, Table 1) also had mixed expression/comprehension language dysfunction near the onset of disease which did not meet formal criteria for primary progressive aphasia. Case #7 exhibited a complex movement disorder which included Parkinsonism, apraxia and eye movement abnormalities. A family history of neurologic or psychiatric disease was present in five of seven cases (Table 1), including case #4 who was found to harbor a hexanucleotide repeat expansion mutation in *C9orf72*. Further genetic analysis was available for cases #1–6 using a next-generation sequencing panel covering of nearly all of the known genetic causes of aging related neurodegenerative diseases including ALS, FTD, Alzheimer's disease, Parkinson's disease and others. No other known disease-causing mutations were identified including *GRN* or *MAPT* mutations. Examination of rare variants of unknown significance did not reveal any consistent genetic alterations or any enrichment of variants within particular disease genes (Table 1). Additional clinical details are available in the supplementary materials.

These seven cases shared a distinct pattern of TDP-43 pathology as revealed by immunohistochemistry of neocortical regions using 1D3, an antibody specific for TDP-43 phosphorylated on serine residues 409 and 410 (Fig. 1). Granulofilamentous neuronal inclusions (GFNI) were present in neocortical neurons which were stained less intensely than more typical compact neuronal cytoplasmic TDP-43 inclusions (Fig. 1a, arrowheads). Morphologically, these inclusions consist of fine granular to thin filamentous structures within neuronal perikarya. Dense, compact neuronal cytoplasmic inclusions (NCI's) were rare to absent. GFNI's were observed in a background of often abundant, very fine grain-like deposits that involved all neocortical layers including layer 1. Moreover, all cases showed curvilinear inclusions in oligodendrocytes within the subcortical white matter (Fig. 1a, Type E—white matter). This pattern of TDP-43 pathology was distinct from the dense neuronal cytoplasmic inclusions (including ring inclusions) and neurites of type A, the compact neuronal cytoplasmic inclusions of type B, the long neuritic profiles of type C, and the numerous neuronal intranuclear inclusions (NII) of type D (Fig. 1a).

To determine the distribution of TDP-43 pathology in these cases, phospho-TDP-43 immunohistochemistry was performed on sections throughout the brain and spinal cord which revealed a surprisingly wide neuroanatomic distribution of TDP-43 pathology. Within the cerebrum (Fig. 1b), GFNI's and grains were seen in frontal, temporal and parietal neocortical areas, although occipital neocortex including primary visual neocortex was

relatively spared with absent to rare TDP-43 aggregates. Oligodendroglial inclusions were readily observed in subcortical white matter, corpus callosum, and the descending corticospinal tracts (Fig. 1b and data not shown). Deep grey structures including hippocampus, amygdala, striatum and thalamus also exhibited GFNI's, grains and oligodendroglial inclusions (Fig. 1b and data not shown). Hippocampal dentate gyrus neurons exhibited some compact NCI's in addition to GFNI's. The amount and intensity of TDP-43 aggregate staining appeared to be sensitive to differential lengths of formalin fixation and the quality of tissue preservation, making comparisons between different cases difficult. Despite this caveat, the amount of TDP-43 pathology within a given case appeared to correlate with the extent of neurodegeneration, most prominently affecting frontal, temporal and anterior cingulate cortical regions.

Phospho-TDP-43 pathology extended into the brainstem and spinal cord (Fig. 1c). TDP-43 aggregates were present in the midbrain including substantia nigra, pons including the basal pontine nuclei, medulla including the medullary olives, and lower motor neurons in the anterior horn of the cervical spinal cord. These affected regions typically exhibited a predominance of GFNI's, grains and oligodendroglial inclusions, although scattered examples of dense, compact TDP-43 inclusions could also be found (arrows, Fig. 1c). While overt neurodegeneration was not obvious in the spinal cord or most of these brainstem structures, the substantia nigra exhibited mild to moderate neuronal loss and gliosis in five of the seven cases including case #7 who exhibited Parkinsonism (Table 1). TDP-43 aggregates were not present in the cerebellum except for very rare oligodendroglial inclusions in two cases (one or two per section).

A semi-quantitative analysis of the density and distribution of TDP-43 pathology is available in the supplementary materials. Additional immunohistochemical analyses demonstrated limited to no tau pathology (Braak stages 0 to II, Table 1). β-amyloid and α-synuclein pathology was absent in all seven cases (data not shown).

To further characterize this distinct pattern of TDP-43 pathology, sections were stained with anti-TDP-43 antibodies that recognize epitopes independent of phosphorylation status. Similar TDP-43 pathology consisting of GFNI's, grains and oligodendroglial inclusions were identified using 6H6E12 (human TDP-43 specific mouse monoclonal antibody, Fig. 1d), 5104 and 5095 (human TDP-43 C-terminus specific mouse monoclonal antibodies, Fig. 1d and data not shown), and C1039 (TDP-43 C-terminus specific rabbit polyclonal antibody, Fig. 2). In addition to confirming the presence of TDP-43 protein within GFNI's, these TDP-43 antibodies demonstrated that GFNI's were often associated with the characteristic clearance of normal nuclear TDP-43 protein in affected neurons (Fig. 1d, open arrowheads).

Despite the detection of aggregates with TDP-43 antibodies, immunohistochemistry using antibodies specific for ubiquitin did not reveal GFNI's, grains or oligodendroglial inclusions (Fig. 1d). To confirm the absence of ubiquitin immunoreactivity within TDP-43 aggregates, double immunofluorescence staining was performed for TDP-43 and ubiquitin which showed that GFNI's, grains and oligodendroglial inclusions were essentially negative for ubiquitin (Fig. 2, Type E). The ubiquitin positive grains seen in Fig. 2 that do not co-localize with TDP-43 pathology likely reflect the aging related emergence of ubiquitin aggregates

during normal aging that are not disease related [8]. To ensure our staining protocol was robust, another FTLD-TDP case was stained concurrently which showed strong ubiquitin immunoreactivity of TDP-43 inclusions typical of most cases of FTLD-TDP (Fig. 2, Type A).

Additional double immunofluorescence was performed on cortical sections for phosphorylated TDP-43 and p62 to determine whether TDP-43 aggregates in these cases colocalized with p62. The vast majority of GFNI's and grains demonstrated very weak to absent immunoreactivity for p62, with scattered (<5%) examples of moderate immunoreactivity (Fig. 3, Type E neuronal, arrowheads). In contrast, oligodendroglial inclusions were consistently and strongly immunoreactive for p62 (Fig. 3, Type E oligodendroglial). Interestingly, p62 immunostaining of a single case (case #5) revealed a moderate density of strongly p62 immunoreactive TDP-43 inclusions which appeared to be astrocytic in morphology (Fig. 3, Type E astrocytic, arrows). Again, to ensure our staining protocol was robust, an FTLD-TDP type B case was stained concurrently which showed that nearly all TDP-43 inclusions were immunoreactive for p62, oftentimes with strong co-localization between phospho-TDP-43 and p62 (Fig. 3, Type B).

Biochemical fractionation of frozen neocortical brain tissue was performed to demonstrate the presence of insoluble and phosphorylated TDP-43 protein. Sarkosyl-insoluble fractions from representative cases of type A, B, C and E were immunoblotted for TDP-43 protein using 5104, a C-terminal TDP-43 antibody, and a p409/p410 phosphorylation-specific antibody (Fig. 4a). Immunoblots revealed the typical biochemical signature associated with FTLD-TDP, namely the presence of phosphorylated TDP-43 protein at ~45 kDa and higher, together with the presence of phosphorylated and C-terminal TDP-43 fragments consisting of three major bands between ~23 and 26 kDa. A subtle difference in the relative abundance of C-terminal fragments was observed in type E cases, where type E cases exhibited a prominent upper C-terminal fragment band of ~26 kDa (Fig. 4a, asterisk) relative to other C-terminal TDP-43 fragments (Fig. 4a, bracket). In contrast, type A, B and C cases showed a predominance of lower C-terminal TDP-43 fragments. Fluorescence-based quantification of band intensities revealed that the upper C-terminal fragment represented ~45.3% of all C-terminal fragments in type E cases, in contrast with ~26.9% for types A, B, and C.

To better characterize this C-terminal fragment, additional immunoblot analysis was performed for six cases where frozen tissue was available with a rabbit polyclonal antibody raised against N-terminal amino acids 1-261 of TDP-43 (10782-AP), together with a p409/p410 phosphorylation-specific TDP-43 antibody (TIP-PTD-P01). The upper C-terminal fragment band was immunoreactive with the 10782-AP antibody (Fig. 4b). Based on epitope mapping of 10782-AP, this result suggests that this upper C-terminal fragment contains residues 203–209 [35]. Notably, other smaller C-terminal fragments were not immunoreactive with 10782-AP, consistent with these smaller fragments exhibiting further N-terminal truncations. Moreover, the upper C-terminal fragment was the predominant C-terminal TDP-43 fragment in all six cases.

Finally, given the distinct pattern of microscopic and biochemical pathology, clinical data were evaluated to determine whether type E cases were associated with a unique clinical

phenotype. Nearly all seven cases were clinically diagnosed with bvFTD, including one case of bvFTD with MND (Table 1). We compared these type E cases with other FTLD-TDP cases. One hundred and nine cases of FTLD-TDP were identified for which clinical data (age of onset and death) and pathologic subtype data were available (n = 38 type A, 34 type B, 30 type C, 7 type E). Insufficient numbers of type D cases were available for analysis. Linear regressions (using type C cases as the reference group) revealed that type E cases exhibited remarkably shorter disease durations (type C: 9.7 ± 4.0 years; Type E: 2.1 ± 1.0 years; mean ± standard deviation; Table 2; Fig. 5a). Type A and B cases also exhibited shorter disease durations relative to type C cases, although the magnitude of this effect was smaller than that observed for type E cases (type A: 6.5 ± 3.5 years; Type B: 7.0 ± 4.3 years; mean ± standard deviation; Table 2; Fig. 5a). The relatively rapid disease progression for type A and B cases is consistent with the enrichment for autosomal dominant forms of FTLD-TDP in these two subtypes (i.e., cases with *GRN* or *C9orf72* mutations).

Age of death was marginally lower for type B and E cases (type A: 68.0 ± 11.0 years; Type B: 67.2 ± 8.0 years; Type C: 72.1 ± 9.3 years; Type E: 63.9 ± 12.3 years; mean ± standard deviation; Table 2; Fig. 5b). No significant differences were observed for age of onset across histologic subtypes (Table 2; Fig. 5c).

Discussion

We identified seven cases of FTLD-TDP based on a distinct pattern of TDP-43 pathology: (1) an overwhelming predominance of GFNI's over compact neuronal inclusions, (2) the presence of abundant, very fine grey matter grains, and (3) the presence of oligodendroglial inclusions. This trio of TDP-43 pathology was negative for ubiquitin, which is typically a hallmark of TDP-43 proteinopathies. Indeed, prior to the discovery of TDP-43 protein in inclusions of FTD and ALS tissues, ubiquitin immunoreactivity was the defining feature of FTLD with ubiquitin-positive, tau-negative, α-synuclein negative inclusions (FTLD-U) [5, 23]. Nearly all of these FTLD-U cases are now known to be TDP-43 proteinopathies, with rare exceptions lacking TDP-43 pathology that were later discovered to harbor FUS inclusions [6, 7, 29, 36]. In addition to the unique morphology of TDP-43 aggregates in these cases, there was a widespread neuroanatomic distribution of pathology. Moreover, clinicopathologic correlations revealed that this histopathologic pattern was uniformly associated with a rapid progression from onset to death.

FTLD-TDP subtypes were originally described by two independent groups, and in large part were based on the use of ubiquitin immunoreactivity [21, 31]. Later, correlations between ubiquitin and TDP-43 immunohistochemistry revealed a high concordance in FTLD-TDP subtyping using either method [7]. In the novel cases described here, TDP-43 aggregates were negative for ubiquitin. Interestingly, Mackenzie et al., commented on cases which appeared similar to other type B cases in the presence of hippocampal pathology but with the pronounced absence of ubiquitin-positive pathology in neocortical regions [21]. It remains possible that the few cases described in our current study are similar to the previously described neocortex-negative cases by Mackenzie et al. [21]. In addition to involving both superficial and deep neocortical layers, others have noted that type B cases can exhibit GFNI's and grains [17, 25]. Moreover, we present one case that exhibited motor

neuron disease and another case that was found to harbor the *C9orf72* repeat expansion mutation. These findings raise the possibility that the cases described here represent a unique subtype of FTLD-TDP type B, or perhaps extreme examples on one end of a spectrum of FTLD-TDP type B. Notably, TDP-43 positive, ubiquitin-negative GFNI's and grains were explicitly not a part of the harmonized classification, and so the relationship between the pathology described here and type B pathology deserves further study [22].

A major strength of the existing FTLD-TDP subtyping criteria lies in the relatively strong association between histopathologic subtypes and various clinical and/or genetic features of disease [6, 9, 10, 17, 21, 22, 28, 31]. The seven cases described here exhibit a common pattern of microscopic pathology, a consistent biochemical signature, and a uniformly rapidly progressive clinical course. Based on this uniformity, we have provisionally categorized these cases as FTLD-TDP, type E, pending independent verification by other groups that this histopathologic pattern is associated with rapidly progressive FTD. Regardless of whether the pattern of pathology presented here is validated as a separate FTLD-TDP type as we propose, or whether these cases lies along a spectrum of FTLD-TDP types, better elucidation of the clinical and genetic associations with GFNI's, grains and oligodendroglial TDP-43 pathology may reveal insights into the pathogenesis of FTLD-TDP. The pathologic, clinical, and genetic features associated with the FTLD-TDP subtypes are summarized in Fig. 6.

GFNI's have been previously called "pre-inclusions" or "early/transitional" inclusions [7, 17, 25, 26]. We avoid these terms now because it is unclear whether GFNI's would progress to form compact neuronal inclusions, or perhaps whether grains would progress to form dense neurites. One possibility is that these ubiquitin-negative aggregates are indeed precursors to more compact or dense, ubiquitinated inclusions, and that these are not seen in the cases described here because death has occurred relatively early after initiation of disease. While most GFNI's and grains were negative for p62, scattered GFNI's and grains were positive for p62 suggesting that acquisition of p62 immunoreactivity precedes ubiquitin modification of TDP-43 aggregates. There was a predominance of the upper C-terminal TDP-43 fragment which perhaps may represent a biochemical signature of relatively immature disease wherein this fragment is further N-terminally truncated over time to generate smaller C-terminal TDP-43 fragments. The implications of this model is that mature, dense inclusions are not required for neurodegeneration, as all cases here exhibited severe clinical phenotypes together with histologic evidence of neurodegeneration in the absence of compact NCI's or dense neurites. Notably, GFNI's can be associated with the clearance of normal nuclear TDP-43 protein which alone may be sufficient to induce neurotoxicity.

Alternatively, this distinct TDP-43 pathology may represent a unique and particularly virulent variant of TDP-43 proteinopathy. Human pathologic staging of neurodegenerative diseases and various basic experimental models support the hypothesis that neurodegenerative disease pathology may transmit from cell to cell in a templated manner that relies on the neuronal connectome [2–4, 14]. The widespread neuroanatomic distribution of TDP-43 pathology suggests that the pathology in these type E cases was capable of rapid transmission through the brain and spinal cord. This is in distinct contrast

with more typical cases of bvFTD or ALS which we described previously as showing more circumscribed neuroanatomic distribution, particularly in early stages of disease [1, 2, 4]. In this model, the distinct morphology, biochemical signature, and rapid clinical course that typify these type E cases reflect a particularly virulent strain of TDP-43 proteinopathy. This possibility awaits a robust experimental model of TDP-43 proteinopathy transmission.

The presence of oligodendroglial inclusions is not unique to type E cases as they are present in other FTLD-TDP subtypes [27]. Moreover, oligodendroglial TDP-43 inclusions have been previously noted to be positive for p62 and negative for ubiquitin as we observed here [15, 27]. The role of oligodendroglial inclusions in FTLD-TDP is unclear, as FTLD-TDP exhibits a predominantly grey matter/neuronal pattern of neurodegeneration. Multisystem atrophy is another neurodegenerative disease which is characterized by abundant oligodendroglial α-synuclein inclusions [12, 34]. Compared to the other α-synucleinopathies (most notably Parkinson's disease, Parkinson's disease dementia, and dementia with Lewy bodies), multisystem atrophy is a clinically aggressive disease with a rapid clinical course [12]. The presence of oligodendroglial inclusions may, therefore, represent the sequelae of a virulent strain of proteinopathy that is capable of transmitting to oligodendrocytes as bystanders. Alternatively, the unique intracellular environment of oligodendrocytes may promote the formation of protein strains which are particularly capable of spreading or inducing neuronal degeneration. Again, the development of experimental models will be vital to discern between these various models.

In summary, we present rare cases of FTLD-TDP which are difficult to subtype based on existing pathologic criteria. We propose that three distinct features (overwhelming predominance of GFNI's, abundance of very fine grey matter grains, presence of oligodendroglial inclusions) may define a new histopathologic subtype, type E, associated with widespread neuroanatomic spread of pathology, a distinct biochemical C-terminal fragment signature, and a rapidly progressive clinical course. The predisposing factors leading to type E pathology are entirely unknown, but histopathologic subtyping (developed prior to the discovery of *GRN* and *C9orf72* mutations in cases of autosomal dominant FTD and/or ALS) has proven to be remarkably good in terms of segregating different genetic forms of FTLD-TDP [6, 9, 10, 17, 21, 22, 28, 31]. Six of the seven cases described here are not associated with any known genetic neurodegenerative disease mutation. However, several cases exhibited strong family histories of either psychiatric or neurologic diseases including dementia, FTD and Parkinsonism, raising the possibility of hitherto unknown genetic mutations. Identifying these unique cases may facilitate future analyses to identify genetic or other predisposing factors which modulate disease pathogenesis.

Supplementary Material

Refer to Web version on PubMed Central for supplementary material.

Acknowledgments

EBL is supported by a Clinical Scientist Development Award from the Doris Duke Chartiable Foundation, and by the National Institutes of Health (R01NS095793 and R21NS097749). Additional support for this study includes National Institutes of Health Grants P30AG10124 and P01AG017586. We thank Maia A. Yoshida for her scientific

illustration, and our patients and their families who made this research possible. We thank Manuela Neumann and Elisabeth Kremmer for providing the phosphorylation-specific TDP-43 antibody 1D3.

References

1. Brettschneider J, Arai K, Del Tredici K, Toledo JB, Robinson JL, Lee EB, Kuwabara S, Shibuya K, Irwin DJ, Fang L, et al. TDP-43 pathology and neuronal loss in amyotrophic lateral sclerosis spinal cord. Acta Neuropathol. 2014; 128:423–437. DOI: 10.1007/s00401-014-1299-6 [PubMed: 24916269]
2. Brettschneider J, Del Tredici K, Irwin DJ, Grossman M, Robinson JL, Toledo JB, Lee EB, Fang L, Van Deerlin VM, Ludolph AC, et al. Sequential distribution of pTDP-43 pathology in behavioral variant frontotemporal dementia (bvFTD). Acta Neuropathol. 2014; 127:423–439. DOI: 10.1007/s00401-013-1238-y [PubMed: 24407427]
3. Brettschneider J, Del Tredici K, Lee VM, Trojanowski JQ. Spreading of pathology in neurodegenerative diseases: a focus on human studies. Nat Rev Neurosci. 2015; 16:109–120. DOI: 10.1038/nrn3887 [PubMed: 25588378]
4. Brettschneider J, Del Tredici K, Toledo JB, Robinson JL, Irwin DJ, Grossman M, Suh E, Van Deerlin VM, Wood EM, Baek Y, et al. Stages of pTDP-43 pathology in amyotrophic lateral sclerosis. Ann Neurol. 2013; 74:20–38. DOI: 10.1002/ana.23937 [PubMed: 23686809]
5. Cairns NJ, Bigio EH, Mackenzie IR, Neumann M, Lee VM, Hatanpaa KJ, White CL 3rd, Schneider JA, Grinberg LT, Halliday G, et al. Neuropathologic diagnostic and nosologic criteria for frontotemporal lobar degeneration: consensus of the consortium for frontotemporal lobar degeneration. Acta Neuropathol. 2007; 114:5–22. DOI: 10.1007/s00401-007-0237-2 [PubMed: 17579875]
6. Cairns NJ, Neumann M, Bigio EH, Holm IE, Troost D, Hatanpaa KJ, Foong C, White CL 3rd, Schneider JA, Kretzschmar HA, et al. TDP-43 in familial and sporadic frontotemporal lobar degeneration with ubiquitin inclusions. Am J Pathol. 2007; 171:227–240. DOI: 10.2353/ajpath.2007.070182 [PubMed: 17591968]
7. Davidson Y, Kelley T, Mackenzie IR, Pickering-Brown S, Du Plessis D, Neary D, Snowden JS, Mann DM. Ubiquitinated pathological lesions in frontotemporal lobar degeneration contain the TAR DNA-binding protein, TDP-43. Acta Neuropathol. 2007; 113:521–533. DOI: 10.1007/s00401-006-0189-y [PubMed: 17219193]
8. Dickson DW, Wertkin A, Kress Y, Ksiezak-Reding H, Yen SH. Ubiquitin immunoreactive structures in normal human brains. Distribution and developmental aspects. Lab Invest. 1990; 63:87–99. [PubMed: 2165197]
9. Forman MS, Mackenzie IR, Cairns NJ, Swanson E, Boyer PJ, Drachman DA, Jhaveri BS, Karlawish JH, Pestronk A, Smith TW, et al. Novel ubiquitin neuropathology in frontotemporal dementia with valosin-containing protein gene mutations. J Neuropathol Exp Neurol. 2006; 65:571–581. [PubMed: 16783167]
10. Geser F, Martinez-Lage M, Robinson J, Uryu K, Neumann M, Brandmeir NJ, Xie SX, Kwong LK, Elman L, McCluskey L, et al. Clinical and pathological continuum of multisystem TDP-43 proteinopathies. Arch Neurol. 2009; 66:180–189. DOI: 10.1001/archneurol.2008.558 [PubMed: 19204154]
11. Giasson BI, Duda JE, Quinn SM, Zhang B, Trojanowski JQ, Lee VM. Neuronal alpha-synucleinopathy with severe movement disorder in mice expressing A53T human alpha-synuclein. Neuron. 2002; 34:521–533. [PubMed: 12062037]
12. Gilman S, Wenning GK, Low PA, Brooks DJ, Mathias CJ, Trojanowski JQ, Wood NW, Colosimo C, Durr A, Fowler CJ, et al. Second consensus statement on the diagnosis of multiple system atrophy. Neurology. 2008; 71:670–676. DOI: 10.1212/01.wnl.0000324625.00404.15 [PubMed: 18725592]
13. Goldman JS, Farmer JM, Wood EM, Johnson JK, Boxer A, Neuhaus J, Lomen-Hoerth C, Wilhelmsen KC, Lee VM, Grossman M, et al. Comparison of family histories in FTLD subtypes and related tauopathies. Neurology. 2005; 65:1817–1819. DOI: 10.1212/01.wnl.0000187068.92184.63 [PubMed: 16344531]

14. Guo JL, Lee VM. Cell-to-cell transmission of pathogenic proteins in neurodegenerative diseases. Nat Med. 2014; 20:130–138. DOI: 10.1038/nm.3457 [PubMed: 24504409]
15. Hiji M, Takahashi T, Fukuba H, Yamashita H, Kohriyama T, Matsumoto M. White matter lesions in the brain with frontotemporal lobar degeneration with motor neuron disease: TDP-43-immunopositive inclusions co-localize with p62, but not ubiquitin. Acta Neuropathol. 2008; 116:183–191. DOI: 10.1007/s00401-008-0402-2 [PubMed: 18584184]
16. Irwin DJ, Cairns NJ, Grossman M, McMillan CT, Lee EB, Van Deerlin VM, Lee VM, Trojanowski JQ. Frontotemporal lobar degeneration: defining phenotypic diversity through personalized medicine. Acta Neuropathol. 2015; 129:469–491. DOI: 10.1007/s00401-014-1380-1 [PubMed: 25549971]
17. Josephs KA, Stroh A, Dugger B, Dickson DW. Evaluation of subcortical pathology and clinical correlations in FTLD-U subtypes. Acta Neuropathol. 2009; 118:349–358. DOI: 10.1007/s00401-009-0547-7 [PubMed: 19455346]
18. Kwong LK, Irwin DJ, Walker AK, Xu Y, Riddle DM, Trojanowski JQ, Lee VM. Novel monoclonal antibodies to normal and pathologically altered human TDP-43 proteins. Acta Neuropathol Commun. 2014; 2:33.doi: 10.1186/2051-5960-2-33 [PubMed: 24690345]
19. Lee EB, Leng LZ, Zhang B, Kwong L, Trojanowski JQ, Abel T, Lee VM. Targeting amyloid-beta peptide (Abeta) oligomers by passive immunization with a conformation-selective monoclonal antibody improves learning and memory in Abeta precursor protein (APP) transgenic mice. J Biol Chem. 2006; 281:4292–4299. DOI: 10.1074/jbc.M511018200 [PubMed: 16361260]
20. Lee EB, Skovronsky DM, Abtahian F, Doms RW, Lee VM. Secretion and intracellular generation of truncated Abeta in beta-site amyloid-beta precursor protein-cleaving enzyme expressing human neurons. J Biol Chem. 2003; 278:4458–4466. DOI: 10.1074/jbc.M210105200 [PubMed: 12480937]
21. Mackenzie IR, Baborie A, Pickering-Brown S, Du Plessis D, Jaros E, Perry RH, Neary D, Snowden JS, Mann DM. Heterogeneity of ubiquitin pathology in frontotemporal lobar degeneration: classification and relation to clinical phenotype. Acta Neuropathol. 2006; 112:539–549. DOI: 10.1007/s00401-006-0138-9 [PubMed: 17021754]
22. Mackenzie IR, Neumann M, Baborie A, Sampathu DM, Du Plessis D, Jaros E, Perry RH, Trojanowski JQ, Mann DM, Lee VM. A harmonized classification system for FTLD-TDP pathology. Acta Neuropathol. 2011; 122:111–113. DOI: 10.1007/s00401-011-0845-8 [PubMed: 21644037]
23. Mackenzie IR, Neumann M, Bigio EH, Cairns NJ, Alafuzoff I, Kril J, Kovacs GG, Ghetti B, Halliday G, Holm IE, et al. Nomenclature for neuropathologic subtypes of frontotemporal lobar degeneration: consensus recommendations. Acta Neuropathol. 2009; 117:15–18. DOI: 10.1007/s00401-008-0460-5 [PubMed: 19015862]
24. McKhann GM, Albert MS, Grossman M, Miller B, Dickson D, Trojanowski JQ. Clinical and pathological diagnosis of frontotemporal dementia: report of the Work Group on Frontotemporal Dementia and Pick's Disease. Arch Neurol. 2001; 58:1803–1809. [PubMed: 11708987]
25. Murray ME, DeJesus-Hernandez M, Rutherford NJ, Baker M, Duara R, Graff-Radford NR, Wszolek ZK, Ferman TJ, Josephs KA, Boylan KB, et al. Clinical and neuropathologic heterogeneity of c9FTD/ALS associated with hexanucleotide repeat expansion in C9ORF72. Acta Neuropathol. 2011; 122:673–690. DOI: 10.1007/s00401-011-0907-y [PubMed: 22083254]
26. Neumann M, Kwong LK, Lee EB, Kremmer E, Flatley A, Xu Y, Forman MS, Troost D, Kretzschmar HA, Trojanowski JQ, et al. Phosphorylation of S409/410 of TDP-43 is a consistent feature in all sporadic and familial forms of TDP-43 proteinopathies. Acta Neuropathol. 2009; 117:137–149. DOI: 10.1007/s00401-008-0477-9 [PubMed: 19125255]
27. Neumann M, Kwong LK, Truax AC, Vanmassenhove B, Kretzschmar HA, Van Deerlin VM, Clark CM, Grossman M, Miller BL, Trojanowski JQ, et al. TDP-43-positive white matter pathology in frontotemporal lobar degeneration with ubiquitin-positive inclusions. J Neuropathol Exp Neurol. 2007; 66:177–183. DOI: 10.1097/01.jnen.0000248554.45456.58 [PubMed: 17356379]
28. Neumann M, Mackenzie IR, Cairns NJ, Boyer PJ, Markesbery WR, Smith CD, Taylor JP, Kretzschmar HA, Kimonis VE, Forman MS. TDP-43 in the ubiquitin pathology of frontotemporal dementia with VCP gene mutations. J Neuropathol Exp Neurol. 2007; 66:152–157. DOI: 10.1097/nen.0b013e31803020b9 [PubMed: 17279000]

29. Neumann M, Sampathu DM, Kwong LK, Truax AC, Micsenyi MC, Chou TT, Bruce J, Schuck T, Grossman M, Clark CM, et al. Ubiquitinated TDP-43 in frontotemporal lobar degeneration and amyotrophic lateral sclerosis. Science. 2006; 314:130–133. DOI: 10.1126/science.1134108 [PubMed: 17023659]

30. Rohrer JD, Guerreiro R, Vandrovcova J, Uphill J, Reiman D, Beck J, Isaacs AM, Authier A, Ferrari R, Fox NC, et al. The heritability and genetics of frontotemporal lobar degeneration. Neurology. 2009; 73:1451–1456. DOI: 10.1212/WNL.0b013e3181bf997a [PubMed: 19884572]

31. Sampathu DM, Neumann M, Kwong LK, Chou TT, Micsenyi M, Truax A, Bruce J, Grossman M, Trojanowski JQ, Lee VM. Pathological heterogeneity of frontotemporal lobar degeneration with ubiquitin-positive inclusions delineated by ubiquitin immunohistochemistry and novel monoclonal antibodies. Am J Pathol. 2006; 169:1343–1352. DOI: 10.2353/ajpath.2006.060438 [PubMed: 17003490]

32. Suh E, Lee EB, Neal D, Wood EM, Toledo JB, Rennert L, Irwin DJ, McMillan CT, Krock B, Elman LB, et al. Semi-automated quantification of C9orf72 expansion size reveals inverse correlation between hexanucleotide repeat number and disease duration in frontotemporal degeneration. Acta Neuropathol. 2015; 130:363–372. DOI: 10.1007/s00401-015-1445-9 [PubMed: 26022924]

33. Toledo JB, Van Deerlin VM, Lee EB, Suh E, Baek Y, Robinson JL, Xie SX, McBride J, Wood EM, Schuck T, et al. A platform for discovery: the University of Pennsylvania Integrated Neurodegenerative Disease Biobank. Alzheimers Dement. 2014; 10(477–484):e471.doi: 10.1016/j.jalz.2013.06.003

34. Trojanowski JQ, Revesz T. Proposed neuropathological criteria for the post mortem diagnosis of multiple system atrophy. Neuropathol Appl Neurobiol. 2007; 33:615–620. DOI: 10.1111/j.1365-2990.2007.00907.x [PubMed: 17990994]

35. Tsuji H, Nonaka T, Yamashita M, Masuda-Suzukake M, Kametani F, Akiyama H, Mann DM, Tamaoka A, Hasegawa M. Epitope mapping of antibodies against TDP-43 and detection of protease-resistant fragments of pathological TDP-43 in amyotrophic lateral sclerosis and frontotemporal lobar degeneration. Biochem Biophys Res Commun. 2012; 417:116–121. DOI: 10.1016/j.bbrc.2011.11.066 [PubMed: 22133678]

36. Urwin H, Josephs KA, Rohrer JD, Mackenzie IR, Neumann M, Authier A, Seelaar H, Van Swieten JC, Brown JM, Johannsen P, et al. FUS pathology defines the majority of tau- and TDP-43-negative frontotemporal lobar degeneration. Acta Neuropathol. 2010; 120:33–41. DOI: 10.1007/s00401-010-0698-6 [PubMed: 20490813]

37. Wood EM, Falcone D, Suh E, Irwin DJ, Chen-Plotkin AS, Lee EB, Xie SX, Van Deerlin VM, Grossman M. Development and validation of pedigree classification criteria for frontotemporal lobar degeneration. JAMA Neurol. 2013; 70:1411–1417. DOI: 10.1001/jamaneurol.2013.3956 [PubMed: 24081456]

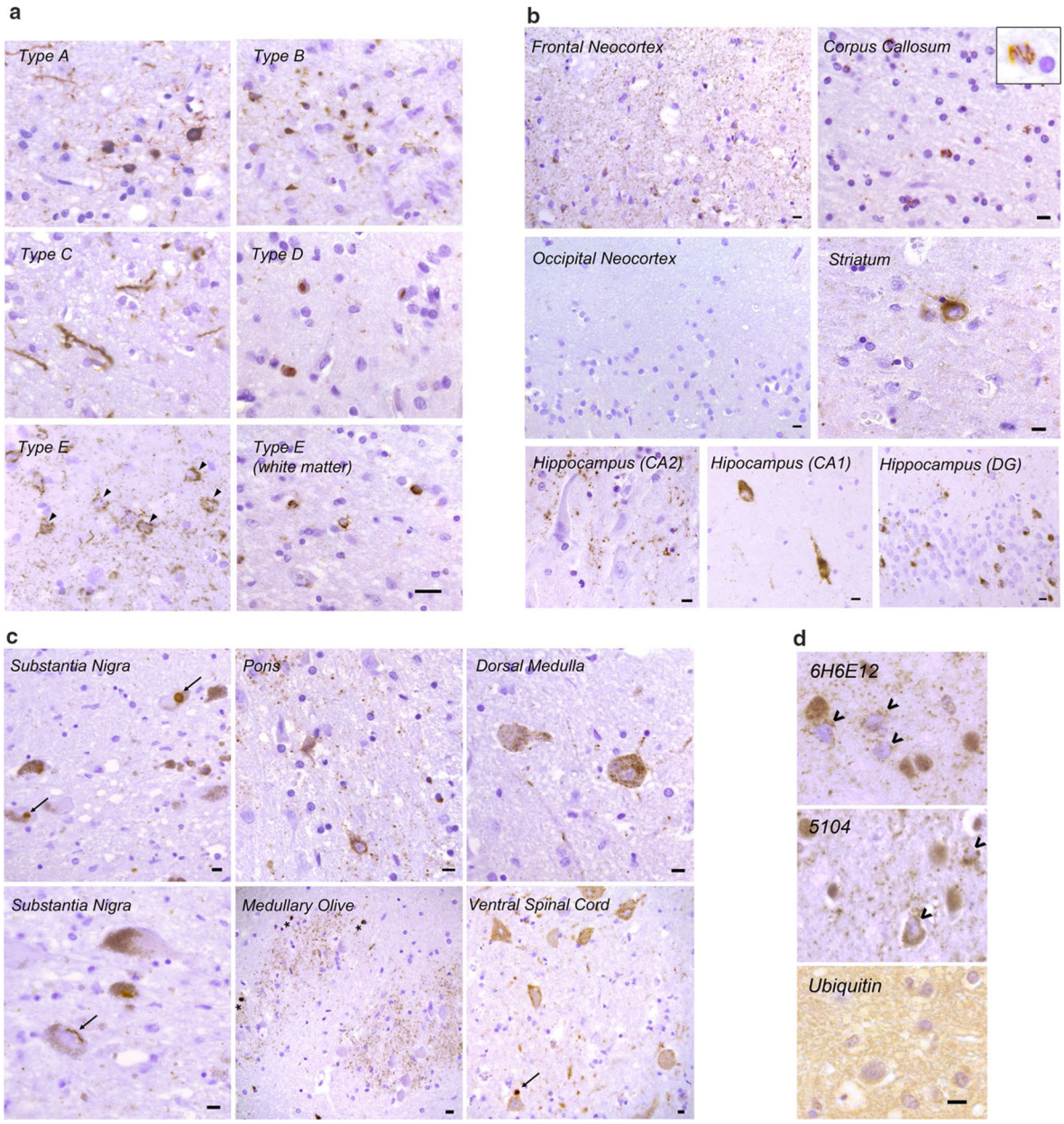

Fig. 1.

Histopathologic characteristics of FTLD-TDP type E. **a** Representative images of p409/p410 immunostained neocortical sections (layer II) from type *A*, *B*, *C*, *D* and E are shown (*scale bar* 20 μm). *Type A* shows dense neuronal cytoplasmic inclusions including ring inclusions, and neurites affecting superficial neocortical layers. *Type B* shows compact neuronal cytoplasmic inclusions with few neurites and involves superficial and deep neocortical layers. *Type C* shows long dystrophic neurites. *Type D* is typified by numerous intranuclear inclusions. *Type E* exhibits GFNI's and grains in superficial and deep neocortical layers. Curvilinear oligodendroglial inclusions are also present (white matter). **b** Type E pathology is seen throughout most of the cerebrum including frontal neocortex, major white matter tracts such as the corpus callosum (inset shows high power image of curvilinear

oligodendroglial inclusion), deep grey structures such as the striatum, and limbic regions such as the hippocampus (DG = dentate gyrus). Also shown is the occipital neocortex which is relatively spared (*scale bars* 10 μm). **c** *Type E* pathology is seen throughout the brainstem and cervical spinal cord. Shown are representative images from the substantia nigra, basis pontis (pons), medullary olive, dorsal medulla and ventral spinal cord. More compact or dense inclusions highlighted with arrows. Oligodendroglial inclusions highlighted with asterisks. *Scale bars* 10 μm. **d** Representative images of type E cases stained with anti-TDP-43 antibodies 6H6E12 and 5104, and the anti-ubiquitin antibody MAB1510 are shown (*scale bar* 10 μm). TDP-43 antibodies reveal both GFNI's and grains with nuclear clearance of normal nuclear TDP-43 in affected neurons (*open arrowheads*). Ubiquitin stain was negative for discernible inclusions

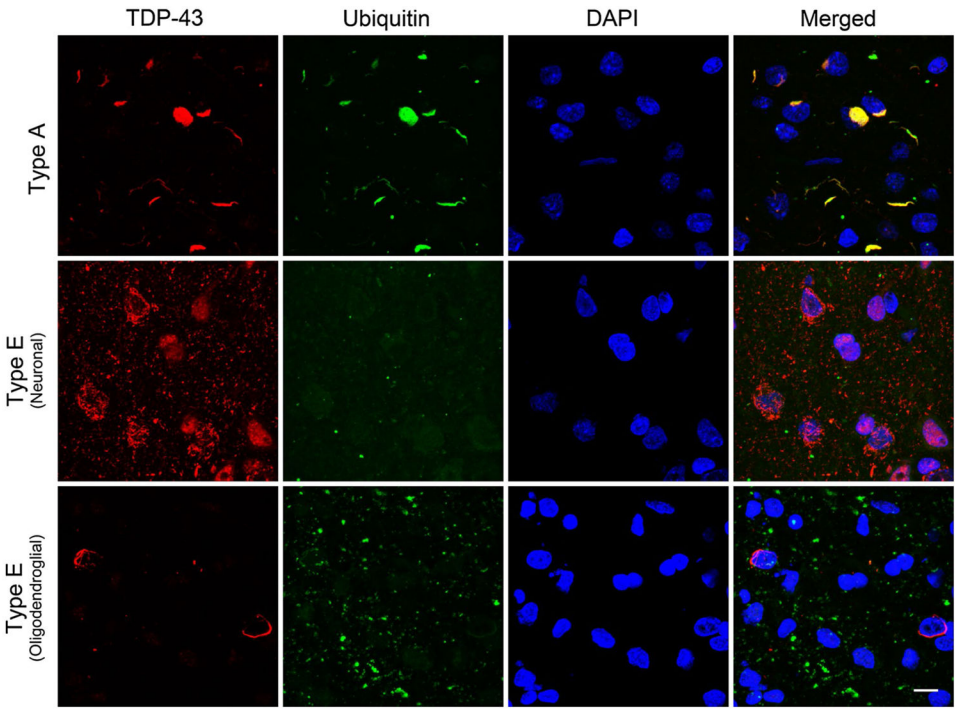

Fig. 2.

TDP-43 positive but ubiquitin-negative inclusions in FTLD-TDP type E. Representative confocal stack images are shown of double immunofluorescence stained cortical sections stained using anti-TDP-43 (C1039, rabbit polyclonal, *red*) and anti-ubiquitin (MAB1510, mouse monoclonal, *green*) with a DAPI nuclear counterstain (*blue*). A typical type A case exhibits inclusions positive for both ubiquitin and TDP-43 positive inclusions (*top panels*). In contrast, neuronal GFNI's and grains from a type E case are TDP-43 positive but ubiquitin negative (*middle panel*). Similarly, curvilinear oligodendroglial inclusions are also TDP-43 positive but ubiquitin negative (*bottom panel*). *Scale bar* 10 μm

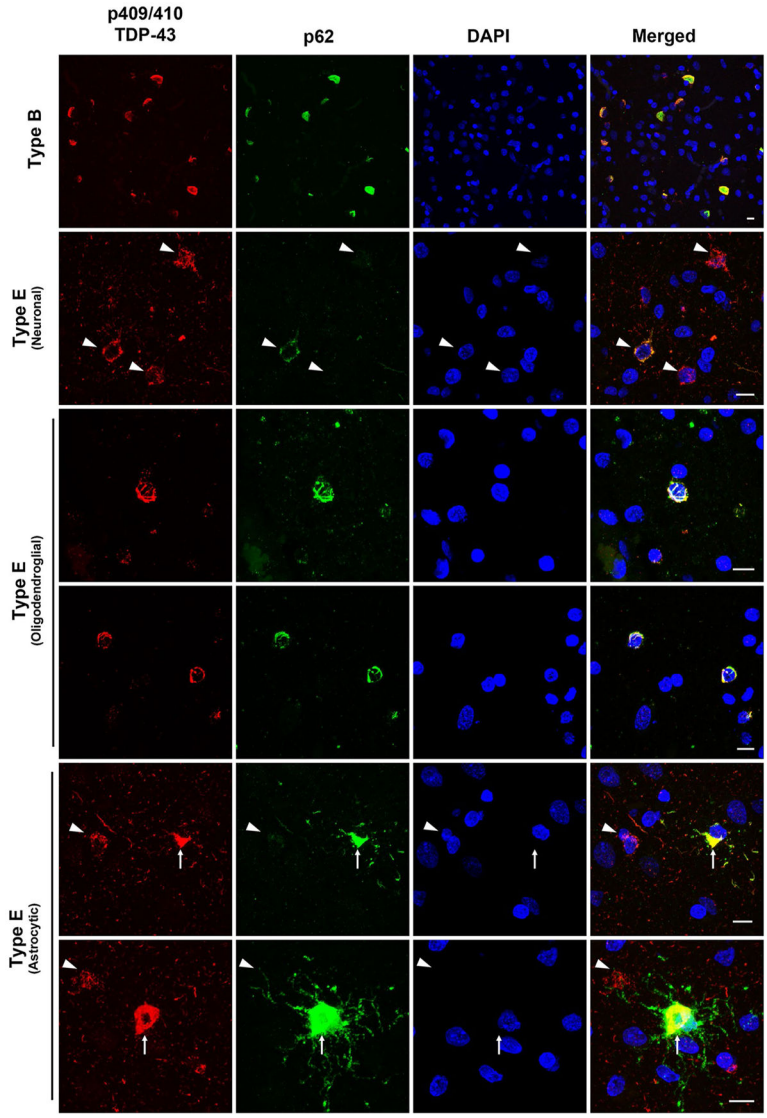

Fig. 3.

TDP-43 positive and variably p62-positive inclusions in FTLD-TDP type E. Representative confocal stack images are shown of double immunofluorescence stained cortical sections stained using anti-p409/410 TDP-43 (TIP-PTD-P01, rabbit polyclonal, *red*) and anti-p62 (2C11, mouse monoclonal, *green*) with a DAPI nuclear counterstain (*blue*). A typical type B case exhibits inclusions positive for both p62 and TDP-43 positive inclusions (*top panels*). In contrast, neuronal GFNI's and grains from a type E case are TDP-43 positive but variably positive for p62 with a small minority of GFNI's exhibiting moderate p62 staining (*upper middle panels*). Curvilinear oligodendroglial inclusions (*middle panels*) and astrocytic inclusion (*bottom panels*) were strongly positive for phospho-TDP-43 and p62. GNFI's are highlighted with *arrowheads*. Astrocytic inclusions are highlighted with arrows. *Scale bars* 10 μm

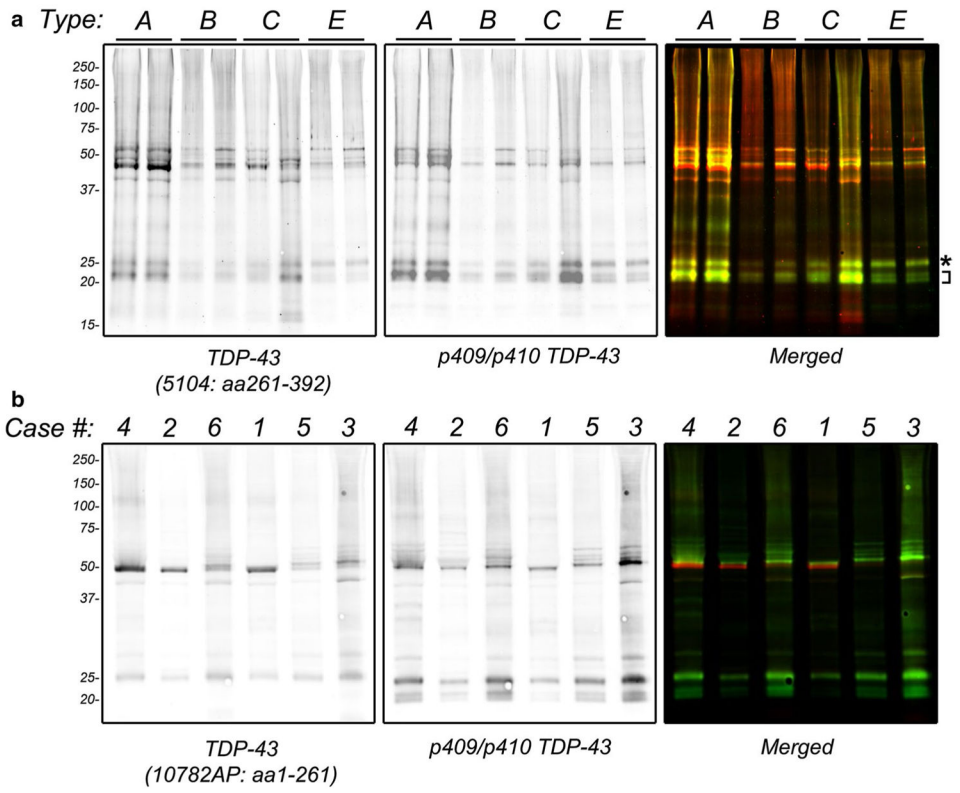

Fig. 4.

Biochemical analysis of FTLD-TDP type E. Frozen frontal cortex from unfixed frozen human brain was subjected to sequential biochemical extraction using a series of buffers of increasing strength. Sarkosyl-insoluble fractions were electrophoresed on NuPage Bis–Tris gels and immunoblotted with primary antibodies as indicated and detected using fluorescently-labeled secondary antibodies followed by dual-color imaging. **a** Representative immunoblot of type *A*, *B*, *C* and *E* cases using 5104 (anti-TDP-43 antibody that recognizes amino acids 261–392, *left panel* and *red* in *right panel*) and TIP-PTD-P01 (anti-p409/p410-TDP-43 antibody that recognizes phosphorylated S409 and S410, *middle panel* and *green* in right panel). *Asterisk* highlights upper C-terminal fragment band. Bracket highlights smaller C-terminal fragments. Sufficient numbers of type D cases were not available for analysis. **b** Immunoblotting of six type E cases (labeled according to Table 1) with 10782-AP (anti-TDP-43 antibody raised against amino acids 1-261, *left panel* and red in *right panel*) and 1D3 (anti-p409/p410-TDP-43, *middle panel* and *green in right panel*)

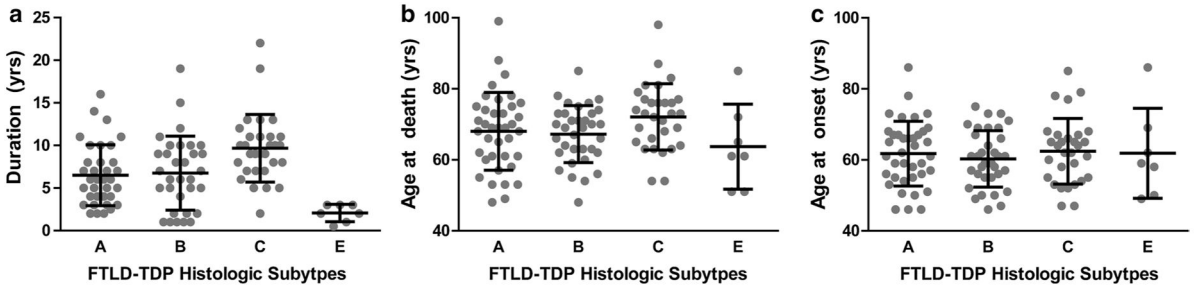

Fig. 5.

FTLD-TDP Subtypes and disease duration, age at death and age at onset. **a** Disease duration, **b** age at death and **c** age at onset are shown for FTLD-TDP type *A*, *B*, *C* and *E* cases. Data presented for each individual together with group mean (*lines*) and standard deviation (*error bars*). Sufficient numbers of *type D* cases were not available for analysis

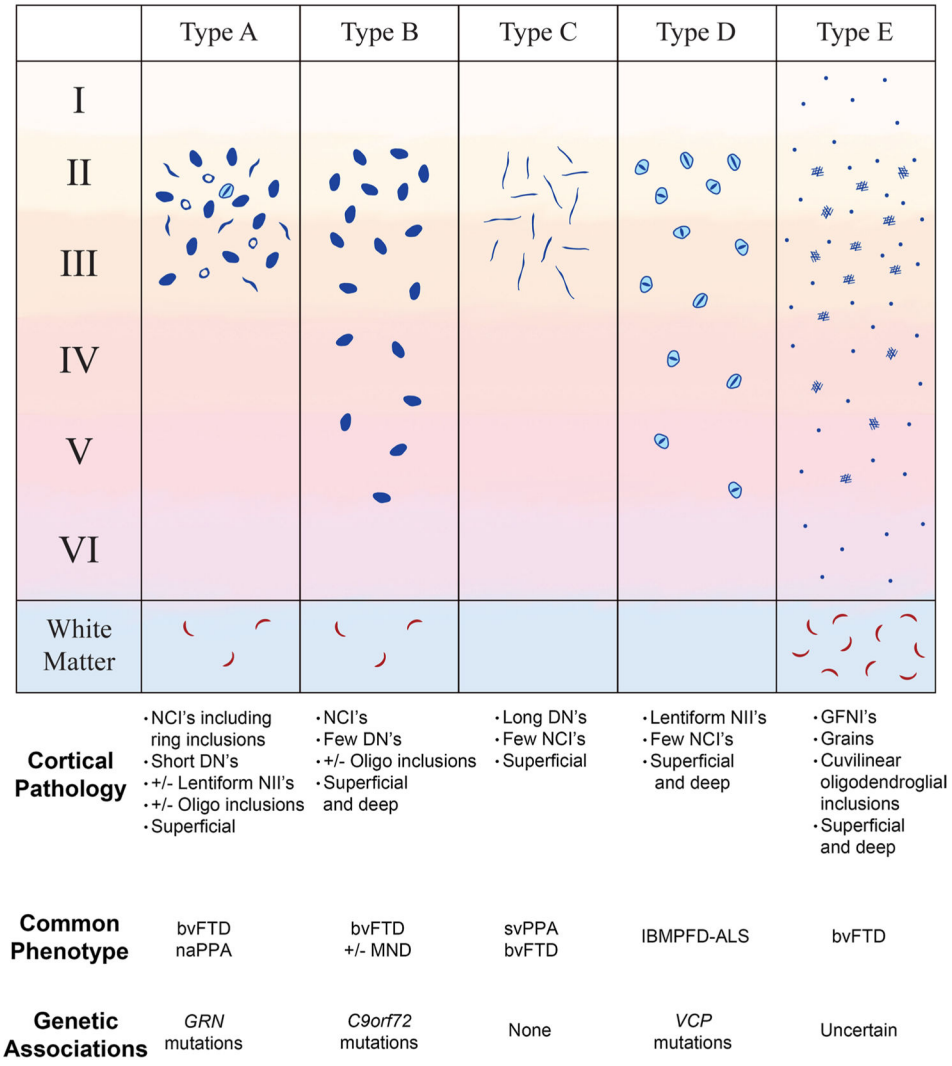

Fig. 6.

Proposed expansion of FTLD-TDP classification. An illustration of TDP-43 aggregate morphology that define Types *A*, *B*, *C*, *D*, and *E* is shown. Below each FTLD-TDP type is a summary of the pathologic features, clinical phenotypes, and genetic features of each subtype. *Type A* is characterized by crescentic to oval/ring-like neuronal cytoplasmic inclusions and many short dystrophic neurites involving superficial neocortical layers. Lentiform neuronal intra-nuclear inclusions and oligodendroglial (oligo) inclusions may also be observed. *Type B* is characterized by neuronal cytoplasmic inclusions affecting superficial and deep neocortical layers with a paucity of dystrophic neurites. Oligodendroglial inclusions may be observed. *Type C* is characterized by long dystrophic neurites predominantly in superficial layers with a paucity of neuronal cytoplasmic inclusions. *Type D* is characterized by frequent lentiform neuronal intranuclear inclusions with short dystrophic neurites. Finally, *Type E* is characterized by granulofilamentous neuronal inclusions and very fine, dot-like neuropil aggregates affecting all neocortical

layers in addition to curvilinear oligodendroglial inclusions in the white matter. Modified from Mackenzie et al. [22]

Table 1

Clinical diagnoses, Braak stage, and rare genetic variants of unknown significance

Case #	Clinical phenotype	Age at onset	Age at death	Braak stage	Family history	Genetics
1	bvFTD	49	51	I	No	*ATXN2* c.957G>A (p.Pro319=) *PSEN1* c.953A>G (p.Glu318Gly)
2	bvFTD/MND	50	51	0	Yes (AD, bipolar disorder, OCD)	*SQSTM1* c.712A>G (p.Lys238Glu) *COQ2* c.64A>T (p.Arg22Ter) *NEFH* c.1387 G>A (p.Glu463Lys)
3	bvFTD	58	61	0	Yes (alcoholism)	*TREM2* c.185G>5 (p.Arg62His) *VCP* c.1704A>G (p.Gln568=) *SETX* c.6507G>A (p.Gly2169=) *SPG11* c.1698T>G (p.Asp566Glu)
4	bvFTD	59	61	II	Yes (ALS, suicide)	*C9orf72* expansion *DCTN1* c.586A>G (p.Ile196Val) *ATP13A2* c.3365C>T (p.Pro1122Leu) *DNAJC13* c.5560+4A>T *DAO* c.108G>A (p.Ala36 =) *EWSR1* c.1408G>A (p.Gly470Ser)
5	bvFTD	62	65	II	No	*LRRK2* c.356T>C (p.Leu119Pro) *PARK7* c.293G>A (p.Arg98Gln) *TMEM106B* c.401G>A (p.Ser134Asn) *NEFH* c.1387G>A (p.Glu463Lys)
6	bvFTD	69	72	I	Yes (PD, FTD)	*ATP13A2* c.3365C>T(p.Pro1122Leu) *PARK2* c.1180G>A (p.Asp394Asn) *SPG11* c.6684C>T (p.Tyr2228=)
7	Parkinsonism/apraxia	85	86	II	Yes (strokes/dementia)	N/A

Family history of neurologic or psychiatric disease is shown with relatives' clinical phenotypes in parentheses

AD Alzheimer's disease, *OCD* obsessive compulsive disorder, *PD* Parkinson's disease

Acta Neuropathol. Author manuscript; available in PMC 2018 July 01.

Table 2

Univariate regression analysis of disease duration, age of death, and age of onset as a function of histologic subtype

	β	St. error	p value	Significance
Duration (R^2 = 0.205)				
Intercept	9.67	0.70	$<2 \times 10^{-16}$	***
Type A	−3.22	0.94	0.000846	***
Type B	−2.70	0.96	0.00572	**
Type E	−7.60	1.60	6.69×10^{-6}	***
Age at death (R^2 = 0.057)				
Intercept	72.10	1.78	$<2 \times 10^{-16}$	***
Type A	−4.07	2.38	0.0904	
Type B	−4.87	2.45	0.0492	*
Type E	−8.24	4.10	0.0468	*
Age at onset (R^2 = 0.009)				
Intercept	62.43	1.65	$<2 \times 10^{-16}$	***
Type A	−0.68	2.21	0.757	
Type B	−2.17	2.26	0.340	
Type E	−0.72	3.79	0.850	